Nonlinear effect of the structured light profilometry in the phase-shifting method and error correction*

Zhang Wan-Zhen(张万祯)[a], Chen Zhe-Bo(陈浙泊)[a)b)], Xia Bin-Feng(夏彬峰)[a)], Lin Bin(林 斌)[a)†], and Cao Xiang-Qun(曹向群)[a)]

[a)] *State Key Laboratory of Modern Optical Instrumentation, CNERC for Optical Instruments, Zhejiang University, Hangzhou* 310027, *China*
[b)] *Hangzhou Dianzi University, Hangzhou* 310007, *China*

(Received 21 August 2013; revised manuscript received 16 September 2013; published online 20 February 2014)

Digital structured light (SL) profilometry is increasingly used in three-dimensional (3D) measurement technology. However, the nonlinearity of the off-the-shelf projectors and cameras seriously reduces the measurement accuracy. In this paper, first, we review the nonlinear effects of the projector–camera system in the phase-shifting structured light depth measurement method. We show that high order harmonic wave components lead to phase error in the phase-shifting method. Then a practical method based on frequency domain filtering is proposed for nonlinear error reduction. By using this method, the nonlinear calibration of the SL system is not required. Moreover, both the nonlinear effects of the projector and the camera can be effectively reduced. The simulations and experiments have verified our nonlinear correction method.

Keywords: structured light profilometry, depth measurement, phase-shifting algorithm, nonlinear effect

PACS: 42.30.–d, 42.30.Rx, 42.30.Kq, 42.30.Wb **DOI:** 10.1088/1674-1056/23/4/044212

1. Introduction

Digital structured light (SL) profilometry is increasingly used in three-dimensional (3D) imaging nowadays because of its fast speed, none contact, and high accuracy nature.[1–4] A classical SL 3D system consists of a digital projector and a camera, which we call the projector–camera system. The projector is used for projecting the SL patterns. From the captured SL patterns, the code words are retrieved based on the decoding algorithm. Then, 3D information can be recovered through triangulation. However, the nonlinear relationship between the projecting SL intensity and the gray value captured in the image has a significant influence on most SL 3D imaging methods. There are two major error sources. One is the gamma phenomenon in off-the-shelf digital projectors,[5,6] and the other is the nonlinearity of digital cameras.[7,8] The problem seriously reduces the accuracy of the SL 3D system.[9,10]

In this paper, a theoretical model of the SL 3D system nonlinearity is analyzed, and a nonlinear correction method based on the Fourier spectrum analysis is proposed. First, we introduce the nonlinear response of the projector–camera system. Then, the influence of nonlinearity on the phase shifting algorithm is discussed. Then, a frequency domain filtering method for nonlinear correction is proposed. By using this method, the nonlinear calibration of the SL system is not required. Moreover, both the nonlinear effect of the projector and camera can be reduced. Finally, both the simulation and experimental results verify the theory and the nonlinear correction method introduced in this paper.

2. Theoretical analysis

2.1. Nonlinear response of a projector–camera system

Ideally, the nonlinear response of a projector–camera system can be illustrated in Fig. 1.

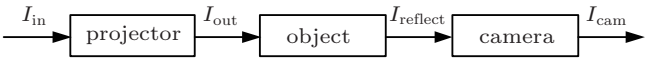


Fig. 1. Nonlinearity of a projector–camera system.

The off-the-shelf digital projector is generally a nonlinear display device for better visual effect. The nonlinearity of a projector can be expressed as

$$I_{\text{out}}(x,y) = I_{\text{in}}(x,y)^{\gamma_1}, \tag{1}$$

where, I_{out} is the intensity of the output light signal; I_{in} is the intensity of the input signal; γ_1 is a constant for a projector.

If the output light is projected onto an object, the reflected light $I_{\text{reflect}}(x,y)$ is

$$I_{\text{reflect}}(x,y) = r(x,y)\left[a(x,y) + I_{\text{out}}(x,y)\right], \tag{2}$$

where $r(x,y)$ is the reflected coefficient, and $a(x,y)$ is the ambient light.

The captured image intensity of the scene $I_{\text{cam}}(x,y)$ is

$$I_{\text{cam}}(x,y) = I_{\text{reflect}}(x,y)^{\gamma_2}, \tag{3}$$

where γ_2 is the nonlinear response of the camera.

*Project supported by the Science and Technology Major Projects of Zhejiang Province, China (Grant No. 2013C03043-5).
†Corresponding author. E-mail: wjlin@zju.edu.cn
© 2014 Chinese Physical Society and IOP Publishing Ltd

2.2. Nonlinear effect in the phase-shifting method

Phase-shifting algorithms have been widely used in optical metrology because of their high measurement accuracy and fast speed.[11] For N-step phase-shifting algorithms with equal phase shifts, the intensity of n-th ($n = 1, 2, \ldots, N$) fringe image $I_n(x,y)$ can be described as

$$I_n(x,y) = B + A\cos\left[\phi(x,y) + 2n\pi/N\right], \tag{4}$$

where B is the background intensity; A is the intensity modulation; $\phi(x,y)$ are the phase code words. The phase $\phi(x,y)$ can be solved as

$$\phi(x,y) = \tan^{-1}\left[\frac{\sum_{n=1}^{N} I_n(x,y)\sin(2n\pi/N)}{\sum_{n=1}^{N} I_n(x,y)\cos(2n\pi/N)}\right]. \tag{5}$$

Because the phase $\phi(x,y)$ is recovered by the arctangent function, its value would stay within the range of $[-\pi, \pi]$. The unwrapped phase value can be obtained using the phase unwrapping method.[12]

For an accurate measurement using the phase-shifting algorithm, ideal sinusoidal fringe patterns are required. However, because of the nonlinearity of the projector–camera system discussed above, the captured fringe patterns for phase recovery are nonsinusoidal. Thus, the measurement accuracy is greatly reduced.

The Fourier series expansion of Eq. (4) can be expressed as

$$\begin{aligned} I_n(x,y) \;=\; & k_0 + k_1\cos\left[\phi(x,y) + 2n\pi/N\right] \\ & + \sum_{m=2}^{M} k_m \cos\left[m\left(\phi(x,y) + 2n\pi/N\right)\right], \end{aligned} \tag{6}$$

where, k_0 is the direct current component; k_1 is the coefficient of the fundamental wave component; k_m is the coefficient of the m-th order harmonic wave. For the sinusoidal fringe pattern, only the first order exists, i.e., k_0 and k_1 are both nonzero, and the coefficients of higher order harmonics are all zero. For nonsinusoidal fringe patterns, the higher order harmonics are all nonzero values. It has been reported that harmonic waves larger than the fifth order seldom exist.[13]

When using the N-step phase-shifting algorithm, Pan *et al.*[13] have shown that the phase error of nonsinusoidal fringe patterns with harmonics up to the fifth-order could be approximated as

$$\Delta\phi(x,y) = -c_3\sin(3\phi(x,y)), \quad \text{for } N = 3; \tag{7}$$

$$\Delta\phi(x,y) = -c_4\sin(4\phi(x,y)), \quad \text{for } N = 4; \tag{8}$$

$$\Delta\phi(x,y) = -c_5\sin(5\phi(x,y)), \quad \text{for } N = 5. \tag{9}$$

Here, $\Delta\phi(x,y)$ is the phase error; c_3, c_4, and c_5 are constants for three-, four-, and five-step phase-shifting algorithms respectively.

Thus, from Eq. (7) to Eq.(9), it can be seen that under the condition of the nonsinusoidal error up to fifth-order harmonic waves, the frequency of the phase error would be 3 times the fringe pitch for the three-step phase-shifting algorithm, 4 times for the four-step method, and 5 times for the five-step method.

2.3. Harmonic filtering for nonlinearity correction

To eliminate the nonlinear phase error, a correction method based on frequency domain filtering is proposed in this section.

Assume that the harmonics higher than order 2 are completely eliminated, the remaining terms are

$$I'_n(x,y) = k_0 + k_1\cos\left[\phi(x,y) + 2n\pi/N\right]. \tag{10}$$

Comparing it with Eq. (4), the only difference between them are the constants k_0 and k_1, which represent the background intensity and the modulation intensity of the sinusoidal signal, respectively. Because the sinusoidal signal term $\cos\left[\phi(x,y) + 2n\pi/N\right]$ is the same as Eq. (4), the ideal phase map can be obtained. This accords well with the previous research result. It has been investigated that for the N-step phase-shifting algorithm, nonlinear harmonic waves up to the $(N-2)$-th order do not affect the phase measurement accuracy.[14,15] Thus, after filtering out harmonic waves higher than the $(N-2)$-th order, the remaining harmonic waves in lower orders do not reduce the accuracy of the N-step phase-shifting algorithm. Because the minimum step number of the phase-shifting method is three, therefore, if the harmonics higher than the first-order are eliminated, the recovered fringe patterns could be used for all N-step number algorithms without error.

Once the corrected phase has been recovered, we can determine the relationship between the nonlinear and linear phase maps. Different from the previous methods,[13,16] the nonlinear correction method we propose here is based on harmonic filtering and the unwrapped phases are stored for the look-up table (LUT). Our method is described as follows.

(i) Use the ideal sinusoidal fringe patterns without precorrection as the SL patterns;

(ii) Project the SL patterns onto a flat board and capture the scene images;

(iii) Filter out harmonic waves higher than the first order in the captured images;

(iv) Recover the phase from both the original and corrected images using the N-step phase-shifting algorithm;

(v) Make the LUT using both unwrapped phases with and without harmonic filtering;

(vi) Use the same SL patterns for object testing and correct the phase error using the LUT.

Note that the unwrapped phase values stored in the LUT are discrete and the continuous values are obtained by spline fitting.

3. Simulation and experiment

To verify the performance of our method, both the simulation and experimental results are given below.

3.1. Simulation

The phase-shifting methods were used for simulation. First, ideal SL patterns were generated according to Eq. (4). Then, nonsinusoidal patterns projected by the projector–camera system were simulated according to Subsection 2.1. In our simulation, both γ_1 and γ_2 are set to be 2.1, and ambient light $a(x,y)$ was set to be 0 for simplification.

The simulation results are shown in Fig. 2. Figure 2(a) shows the intensity curves of the ideal sinusoidal fringe (the solid curve) and the nonsinusoidal fringe affected by the nonlinear projector–camera system (the dash curve). Figures 2(b) and 2(c) show the Fourier spectrum of the ideal sinusoidal fringe and the nonsinusoidal fringe respectively. It can be clearly seen that, the spectrum of sinusoidal fringe has only a direct current component and the fundamental wave components. But, the spectrum of the nonsinusoidal fringe has higher order harmonic components. Given in Fig. 2(d) are the wrapped phase curves obtained by using different phase shifting methods. We can see that the phase curve of the sinusoidal fringe is linear in a wrapped period. For the nonsinusoidal fringe, the phase curve becomes nonlinear. Moreover, the nonlinear phase curve has N waves in a wrapped period, where N is the step number in the phase-shifting method. This verifies the error function Eq. (7) discussed above. In Fig. 2(e), the unwrapped curves of the phase curves are shown. The phase errors are given in Fig. 2(f). The periods of the error curves in Fig. 2(f) accord well with the theoretical values.

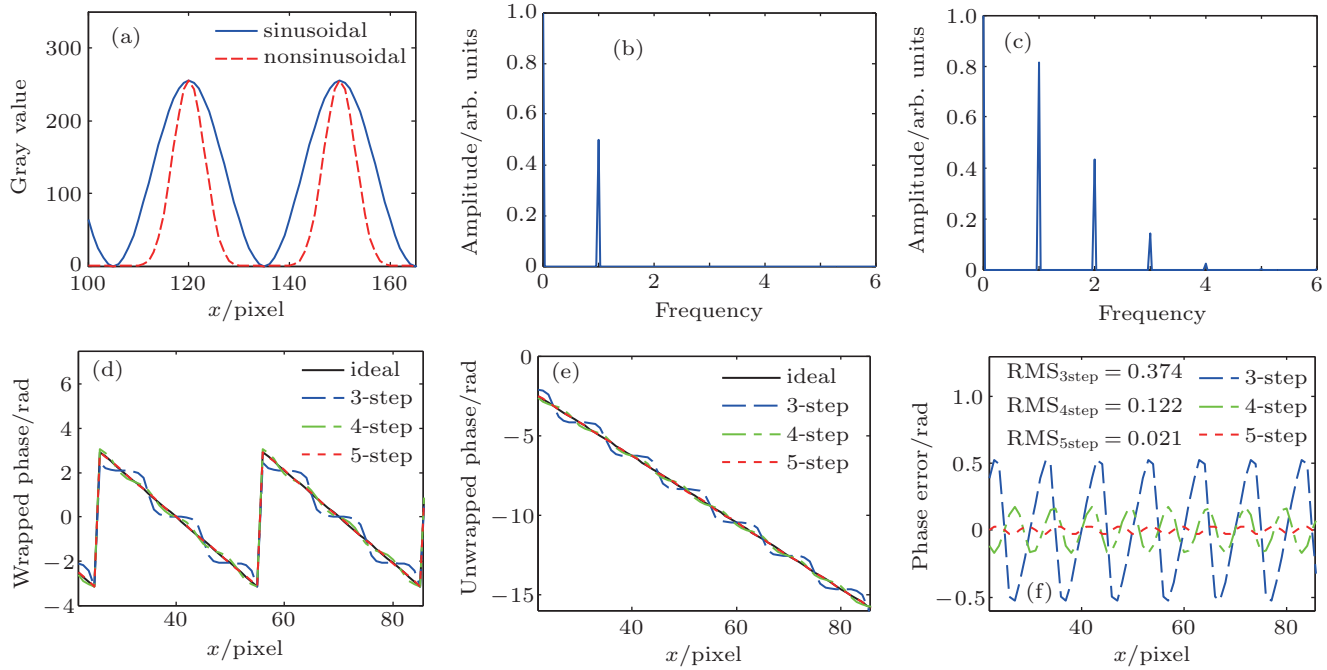


Fig. 2. (color online) Simulations for the nonlinear effect of the projector–camera system, showing (a) intensity curves of patterns, (b) spectrum of a sinusoidal pattern, (c) spectrum of a nonsinusoidal pattern, (d) wrapped phase curves, (e) unwrapped phase curves, and (f) phase error curves.

The harmonic components filtering are simulated as well. We first eliminate the harmonic components higher than the first order, then recover the image using the inverse Fourier transform. The spectrum after filtering can be seen in Fig. 3(a). Only the zero- and the first-order components are left in Fig. 3(a). Then, the recovered image can be processed using the phase-shifting method. The wrapped and unwrapped phase curves are shown in Figs. 3(b) and 3(c) respectively. As demonstrated, all the phase curves are straight without waves now. In order to verify the linearity property, the difference between the ideal unwrapped phase and the corrected one is calculated. The result in Fig. 3(d) shows that the phase error disappears, and root mean squares (RMSs) of all the three phase-shifting methods are zero. Thus, the filtered fringes can be used for accurate 3-, 4-, and 5-step phase-shifting methods. Note that in simulation, there is no environment error, thus the high order harmonics can be easily filtered out, and thus result in no phase error. But, two major error sources exist in experiment. One is the harmonic spectrums overlapping,[7,17] and the other is the complex spectrum of irregular deformed fringes. Therefore, in experiment, undesired harmonics cannot be completely eliminated and phase error exists. The location of the phase jumping points in the wrapped phase map may shift because of the phase error there.

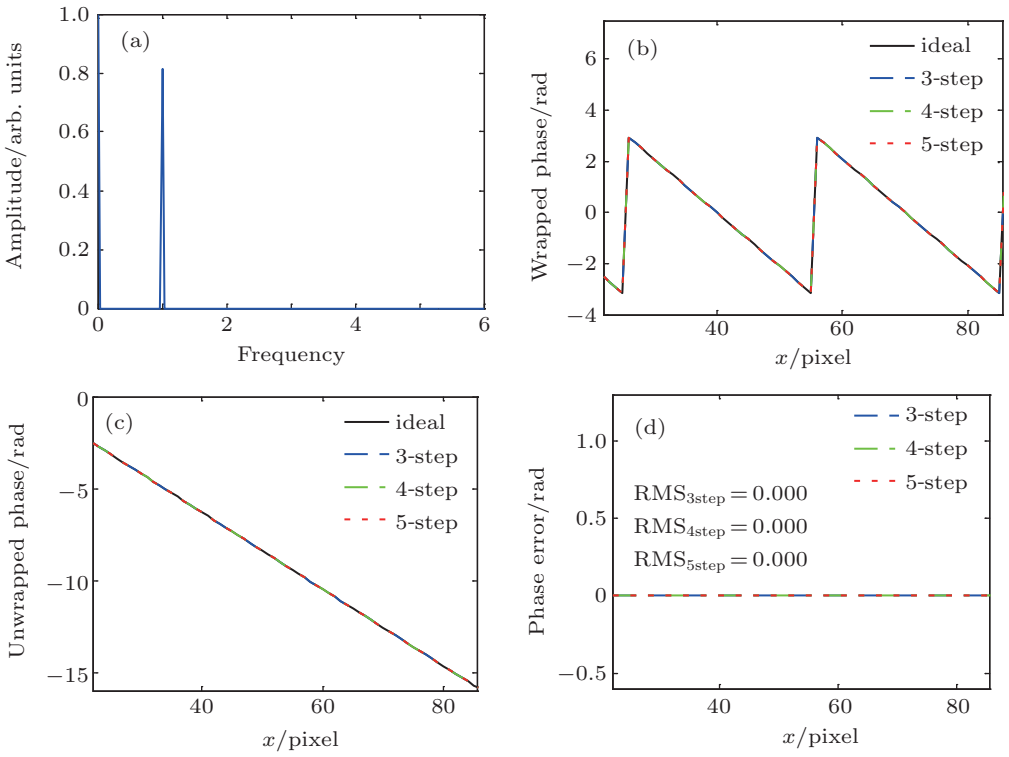


Fig. 3. (color online) Simulation results for the harmonic filtering nonlinearity correction method, showing (a) spectrum after harmonic filtering, (b) phase retrieved, (c) unwrapped phase, and (d) phase error.

3.2. Experiment

To further verify our method, experiments have been carried out.

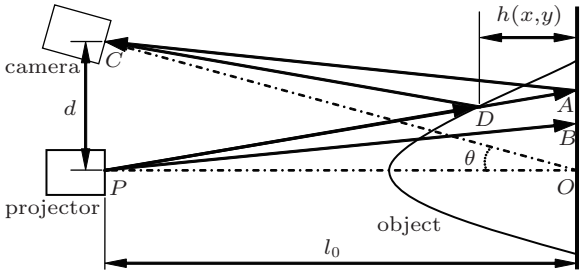


Fig. 4. Schematic diagram of the experimental system.

Figure 4 illustrates the schematic diagram of our experimental system, which consists of an LCoS projector (Esonic HD-720P) and a digital CCD camera (AVT Manta G-031B) with an 8-mm focal length Megapixel lens (Computar M0814-MP2). The resolution of our camera is 640×480. The projector has a resolution of 1280×720 with a projection distance of 0.3 m–5.5 m. In our system, crossed-optical-axes geometry is used. The crossing angle of two optical axes θ is about 75°. There is a separation d of about 250 mm between the camera and the projector. The reference plate distance l_0 is about 650 mm. The 3-, 4-, and 5-step phase-shifting methods are used in our experiment. The fringe pitch of the pattern is 30 pixels. Sinusoidal SL pattern signals without pre-correction are sent to the projector, and the SL modulated scenes are captured by the camera.

First, harmonic wave filtering is carried out for nonlinear correction according to the method discussed above. Then, both the captured images and the recovered image are used for phase retrieval. After the phase unwrapping, the LUT is established for error reduction.

Figure 5 demonstrates the nonlinear correction results. Note that to make the error waves more visible, a gamma value of 2.1 has been preset in the SL patterns to enhance the nonlinear effect. Figure 5(a) is one of the captured fringe patterns, whose Fourier spectrum is shown in Fig. 5(b). It shows that harmonic waves up to the 3rd-order are relatively large, and higher order harmonics in the insert figure are relatively small. Figure 5(d) shows the recovered pattern after filtering out the harmonic components. Figure 5(e) is the Fourier spectrum of Fig. 5(d), only the zero- and the first-order harmonics remain. The inset in Fig. 5(d) shows that the high order harmonics are clearly eliminated. The captured images and recovered images are used for phase retrieval and the obtained phase curves are shown in Figs. 5(c) and 5(f), respectively. It is clear that the wrapped phase curve after harmonic filtering is largely linearized. The unwrapped phases are shown in Figs. 5(g) and 5(h). The phase difference is presented in Fig. 5(i). Again here, the period frequency of the error curve is about N times the pattern fringes, where N is the step number in the phase-shifting method.

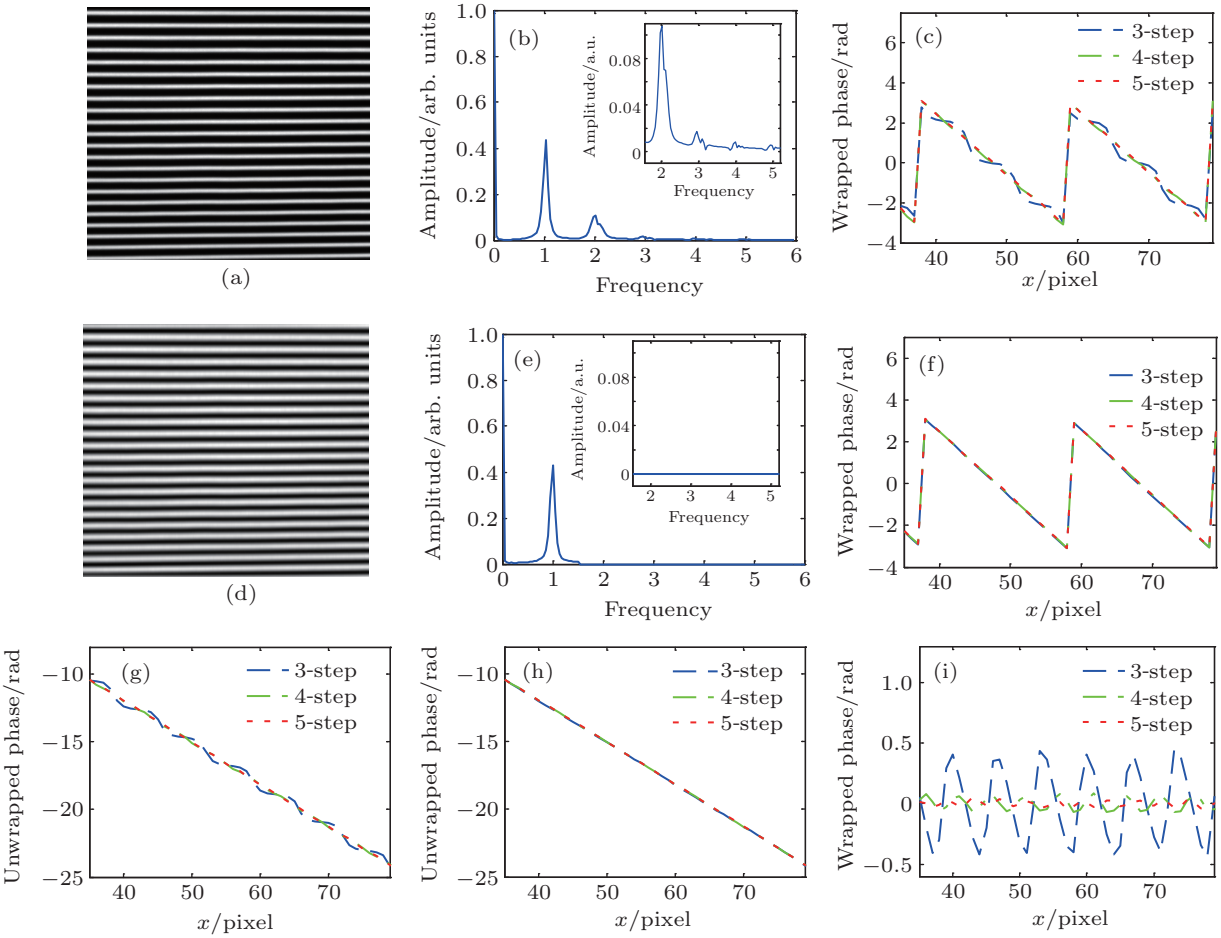


Fig. 5. (color online) Experimental results for nonlinear correction, showing (a) a captured fringe pattern, (b) spectrum of panel (a), (c) phase retrieved, (d) a pattern recovered, (e) spectrum of panel (d), (f) phase retrieved from patterns recovered, (g) and (h) unwrapped phase from panels (c) and (f) respectively, and (i) phase difference, a.u. is the abbreviation for arbtrary units.

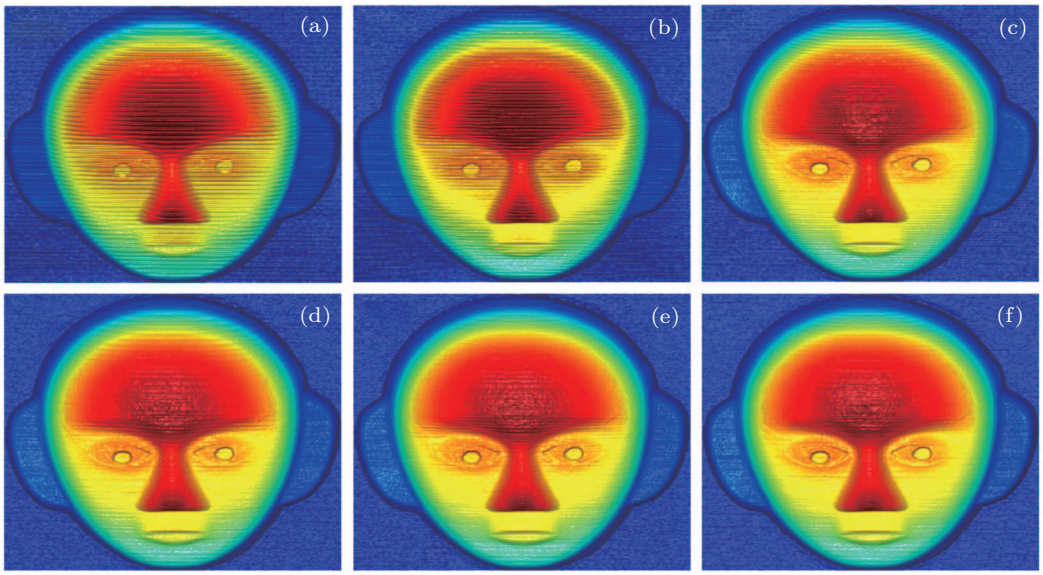


Fig. 6. (color online) Object measurement results. (a)–(c) Depth obtained using 3-, 4-, and 5-step method; (d)–(f) Depth recovered from panels (a)–(c) using our nonlinearity correction method.

In order to further verify our method, the profile of a mask is measured and then corrected using the LUT method. The reference plane method is used for depth recovery.[18] The measurement results are shown in Fig. 6. Figures 6(a)–6(c) show the recovered depth maps without nonlinear correction. There are noticeable ripples on the mask in Figs. 6(a) and 6(b),

which represent serious errors; further, only faint outlines of the mask can be seen in these two figures. Figures 6(d)–6(f) are the depth maps recovered from Figs. 6(a)–6(c) by our nonlinear correction method using the LUT. The ripples almost disappear in these figures and the details of the mask can be seen now. Thus, after our nonlinear correction, the measurement result is improved.

4. Conclusions

We discussed the nonlinear effect of the projector–camera system in phase-shifting SL depth imaging technology, and a practical method was proposed to reduce the error caused by it. We found that both the gamma phenomenon of the projector and the camera contribute to the projector–camera system nonlinearity, and the nonlinearity of the system leads to nonsinusoidal fringe patterns, which have high order harmonic components. For the N-step phase-shifting method, the harmonics higher than the $(N-2)$-th order result in phase recovery errors.

A nonlinear correction method was also proposed in this paper. By eliminating the harmonic components higher than the first-order, the recovered fringe patterns can be used for any N-step phase-shifting method without phase reconstruction error and an LUT method can effectively correct the nonlinearity in the measured object. By using this method, the parameters of the projector–camera system are not required. Both the simulation results and experimental results have verified the nonlinearity error theory and our correction method.

References

[1] Zhang Q C and Su X Y 2013 *International Conference on Optics in Precision Engineering and Nanotechnology*, June 22, 2013, Singapore, Singapore, p. 87691H
[2] Gorthi S and Rastogi P 2010 *Opt. Laser Eng.* **48** 133
[3] Zhang S, Gong Y, Wang Y J, Laughner J and Efimov I 2010 *International Symposium on Optomechatronic Technologies (ISOT),* October 25, 2010, Toronto, Canada, p. 1
[4] Qiao N S, Cai X H and Yao C M 2009 *Chin. Phys. B* **18** 4881
[5] Zhang C, Huang P S and Chiang F 2002 *Appl. Opt.* **41** 5896
[6] Poynton C 1993 *Society of Motion Pic. Tel. Engineers* **102** 1099
[7] Qiao N S and Zou B J 2013 *Chin. Phys. B* **22** 014203
[8] Creath K 1992 *Int. Symp. on Optical Fabrication, Testing, and Surface Evaluation*, June 10, 1992, Tokyo, Japan, p. 428
[9] Guo H, He H and Chen M. 2004 *Appl. Opt.* **43** 2906
[10] Li Z and Li Y 2011 *Opt. Lett.* **36** 154
[11] Malacara D 2007 *Optical Shop Testing*, 3rd edn. (New Jersey: Wiley-Interscience)
[12] Ghiglia D C and Pritt M D 1998 *Two-Dimensional Phase Unwrapping: Theory, Algorithms, and Software* (New York: Wiley)
[13] Pan B, Kemao Q, Huang L and Anand A 2009 *Opt. Lett.* **34** 416
[14] Hoang T, Pan B, Nguyen D and Wang Z Y 2010 *Opt. Lett.* **35** 1992
[15] Stetson K A and Brohinsky W R 1985 *Appl. Opt.* **24** 3631
[16] Zhang S and Yau S 2007 *Appl. Opt.* **46** 36
[17] Wang D J and Zhang T 2011 *Chin. Phys. B* **20** 087202
[18] Srinivasan V, Liu H C and Halioua M 1984 *Appl. Opt.* **23** 3105